

OPEN ACCESS

A Design of Experiments (DOE) approach to optimise temperature measurement accuracy in Solid Oxide Fuel Cell (SOFC)

To cite this article: F Barari *et al* 2014 *J. Phys.: Conf. Ser.* **547** 012004

View the [article online](#) for updates and enhancements.

Related content

- [R1234yf vs. R134a Flow Boiling Heat Transfer Inside a 3.4 mm ID Microfin Tube](#)
A Diani, S Mancin and L Rossetto
- [Theoretical analysis of screened heat pipes for medium and high temperature solar applications](#)
P Di Marco, S Filippeschi, A Franco *et al.*
- [Numerical simulation of turbulent forced convection in liquid metals](#)
S Vodret, D Vitale Di Maio and G Caruso

Recent citations

- [Multi-Response Optimization of Mechanical Properties of Hybrid \(Fiberglass / Abaca Woven\) in Polyester Matrix using Desirability Function based on DOE](#)
J Paredes *et al*
- [Characterizing membrane electrode assemblies for high temperature polymer electrolyte membrane fuel cells using design of experiments](#)
Yasser Rahim *et al*



IOP | ebooks™

Bringing you innovative digital publishing with leading voices to create your essential collection of books in STEM research.

Start exploring the collection - download the first chapter of every title for free.

A Design of Experiments (DOE) approach to optimise temperature measurement accuracy in Solid Oxide Fuel Cell (SOFC)

F Barari^{1,2}, R Morgan¹ and P Barnard²

¹University of Brighton, Cockcroft Building, Lewes Road, Brighton, BN2 4GJ, UK

²Ceres Power Limited, Viking House, Foundry Lane, Horsham RH13 5PX, UK

E-mail: farzad.barari@cerespower.com

Abstract. In SOFC, accurately measuring the hot-gas temperature is challenging due to low gas velocity, high wall temperature, complex flow geometries and relatively small pipe diameter. Improper use of low cost thermometry system such as standard Type K thermocouples (TC) may introduce large measurement error. The error could have a negative effect on the thermal management of the SOFC systems and consequential reduction in efficiency. In order to study the factors affecting the accuracy of the temperature measurement system, a mathematical model of a TC inside a pipe was defined and numerically solved. The model calculated the difference between the actual and the measured gas temperature inside the pipe. A statistical Design of Experiment (DOE) approach was applied to the modelling data to compute the interaction effect between variables and investigate the significance of each variable on the measurement errors. In this study a full factorial DOE design with six variables (wall temperature, gas temperature, TC length, TC diameter and TC emissivity) at two levels was carried out. Four different scenarios, two sets of TC length (6 – 10.5 mm and 17 – 22 mm) and two different sets of temperature range (550 – 650 °C and 750 – 850 °C), were proposed. DOE analysis was done for each scenario and results were compared to identify key parameters affecting the accuracy of a particular temperature reading.

1. Introduction

Accurate measurement of the gas temperature is vital for thermal management of SOFC system. Temperature measurement error could have a detrimental effect on system overall efficiency, reduce system life and may even cause a complete system failure. In addition, running the system outside of the material safe operating temperature range may generate toxic gas or hazardous material. An expensive sophisticated thermometry system may improve the system performance but this is not a practical option for manufacturing this system at a competitive price in high volume. Challenges arose when a low cost, robust and accurate thermometry system is needed for SOFC systems.

A K-type TC is a simple and inexpensive thermometry sensor with a reasonable accuracy. It is widely used in industry for high temperature measurement. However, a common mistake is to simply place a TC into a small diameter pipe to measure a gas temperature. The problem exacerbates when it is used in high temperature dynamic system like SOFC. A common problem of measuring hot-gas temperature inside a pipe is ignoring the effects of thermal radiation emitted by the surrounding as well as the heat conduction from the wall via the TC stem [1]. This may introduce systematic temperature measurement errors. The effect of thermal conduction and radiation on TC measurements



accuracy has been investigated several times mainly in gas turbine, combustors and fire studies [2-7]. However, the dominant effect in this type of measurement has not been clearly identified.

In this study, a one-dimensional mathematical model was developed to investigate the effect of heat conduction, convection and radiation on temperature measurement with a thermocouple attached to a wall. Since there were six major factors influencing the temperature measurement, Design of Experiment (DOE) method was used to determine the effect of critical factors and their interaction. Four different temperature measurement scenarios were proposed. A full factorial DOE was designed at two levels for each scenario and the results were analysed and plotted by Minitab software.

2. Mathematical model

The aim of measuring gas temperature is to measure the gas thermal energy via convection. However, heat transfers from the adjacent components via radiation and conduction could affect the temperature measurement. In fact, the temperature measurement is a result of heat balance on the TC stem [1]. For instance, if the wall temperature is higher than the gas temperature, heat transfers from the wall to the tip via conduction and the wall radiates heat to the TC stem and tip.

In this study the TC is considered to be a cylindrical probe immersed to a gas stream inside a pipe. It was assumed that the gas steam is uniform in terms of velocity (non-viscous fluid) and temperature across the pipe. The pipe wall was assumed to be at a constant temperature (no thermal gradient). There was no thermal resistance at the junction between the TC and the wall. A perfect thermal contact between the TC and the wall is not realistic assumption. However, the actual thermal resistance is depends on several factors such as fitting martial, contact force between the TC fitting and TC, method of attaching fitting to the wall and wall material. Therefore, a perfect thermal contact assumption was simplified the analysis and reduced the ambiguity regarding the thermal conductivity between the TC and wall.

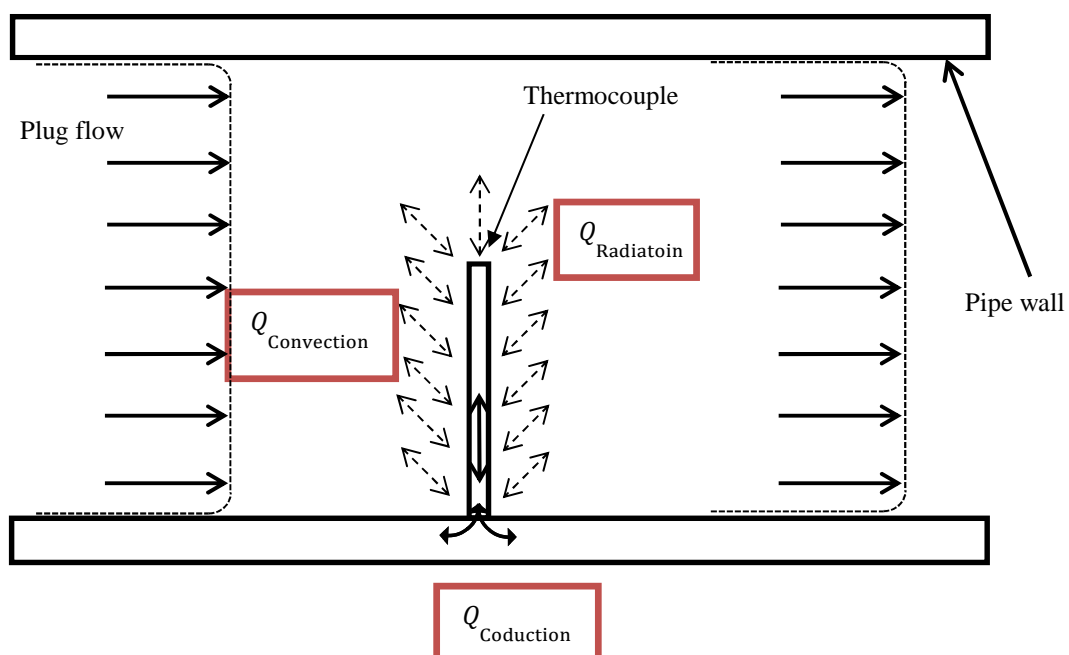


Figure 1. Schematic view of a thermocouple in a pipe subjected to a gas stream.

A 1-D energy balance equation describes the heat balance for this system. It can be seen from equation 1 that the left term is the heat that accumulate on the TC. On the right-hand side are the three terms that transfers heat to/from the TC.

$$\underbrace{\rho_{TC} C_{TC} \frac{dT_{TC}(x)}{dt}}_{\text{heat accumulation on TC}} = \underbrace{k_{TC} \frac{d^2 T_{TC}(x)}{dx^2}}_{\text{Conduction}} - \underbrace{\frac{4}{D_{TC}} h (T_{TC}(x) - T_g)}_{\text{Convection}} - \underbrace{\frac{4}{D_{TC}} F \sigma (T_{TC}^4(x) - T_w^4)}_{\text{Radiation}} \quad (1)$$

where ρ is the density, k is the thermal conductivity, t is time, T is temperature D_{TC} is the TC diameter, h is convection heat transfer coefficient, σ is the Stefan-Boltzmann constant and F is radiation transfer factor.

It can be seen from the equation 2 that the Nusselt number (Nu) and gas thermal conductivity (k_g) should be calculated in order to estimate h .

$$h = Nu \frac{k_g}{D_{TC}} \quad (2)$$

The Nusselt number was calculated based on a cross flow over a cylinder (equation 3) [8]. This equation is valid for Reynolds numbers (Re_D) ≤ 4000 and Prandtl numbers (Pr) ≥ 0.2

$$Nu = 0.3 + \frac{0.62 Re_D^{1/2} Pr^{1/2}}{\left[1 + \left(\frac{0.4}{Pr}\right)^{2/3}\right]^{1/4}} \left[1 + \left(\frac{Re_D}{282000}\right)^{5/8}\right]^{4/5} \quad (3)$$

The gas thermal conductivity was calculated by fitting a line to Kadoya and Matsunaga experimental data [9]:

$$k_{air} = Tg \ 6 \times 10^{-5} + 0.0077 \quad (4)$$

Gas viscosity (μ) was calculated with Sutherland's law:

$$\mu = \mu_{ref} \left(\frac{T}{T_{ref}}\right)^{3/2} \frac{T_{ref} + S}{T + S} \quad (5)$$

where S is Sutherland's constant which is 120 for air.

It was assumed that the TC was a small grey body enclosed in a larger body (pipe) with hypothetically homogeneous temperature (wall temperature). As a result, the transfer factor (F), can be simplified to the TC emissivity [8]:

$$F = \frac{1}{\frac{1}{\varepsilon_{TC}} + \frac{A_{TC}}{A_w} \left(\frac{1}{\varepsilon_{TC}} - 1\right)} \quad (6)$$

$$A_w \gg A_{TC} \therefore F \cong \varepsilon_{TC}$$

Following boundary conditions were used to solve equation 1:

$$T_{TC}(0) = T_w \tag{7}$$

$$\frac{dT_{TC}}{dx} = 0 @ x = L_{TC} \tag{8}$$

3. Numerical solution:

The exact solution for a steady state version of equation 1 is available in literature [10]. Since SOFC systems are dynamic systems and pipes temperature varies at different electric loads, it is important to know the transient time to accurately control the systems. For a transient condition, analytical solution is more complicated and numerical solution is more favourable than the analytical one. The transient effect on temperature measurement accuracy is dependent on several factors such as start-up, shutdown and electric load profile of SOFC systems. Therefore it is not practical to add this factor to DOE analysis and this effect is not considered in this paper.

The equation was solved by the implicit Backward-Time Centred-Space (BTCS) method. In this method the time derivative part of the equation was replaced by the first-order backward-time finite difference approximations and the distance derivative part was replaced by the second-order centred-space approximation and they were evaluated at the solution time level n+1.

$$\frac{d^2T(x)}{dx^2} \cong \frac{T_{i+1}^{l+1} - 2T_i^{l+1} + T_{i-1}^{l+1}}{\Delta x^2} \tag{9}$$

$$\frac{dT(x)}{dt} = \frac{T_i^{l+1} - T_i^l}{\Delta t} \tag{10}$$

Substituting equation 9 and 10 in equation 1 yields equation 11:

$$\rho_{TC} C_{TC} \frac{T_i^{l+1} - T_i^l}{\Delta t} = k_{TC} \frac{T_{i+1}^{l+1} - 2T_i^{l+1} + T_{i-1}^{l+1}}{\Delta x^2} - \frac{4}{D_{TC}} h (T_i^l - T_g) - \frac{4}{D_{TC}} \sigma (T_i^{l4} - T_w^4) \tag{11}$$

After introducing λ , a and b , equation 11 can be rewrite as equation 12.

$$\lambda = \frac{k_{TC} \Delta t}{\rho_{TC} C_{TC} \Delta x^2} \quad a = \frac{4 \Delta t h}{\rho_{TC} C_{TC} D_{TC}} \quad b = \frac{4 \Delta t \epsilon_{TC}}{\rho_{TC} C_{TC} D_{TC}}$$

$$(1 + 2\lambda)T_i^{l+1} - \lambda T_{i-1}^{l+1} - \lambda T_{i+1}^{l+1} = -aT_i^l - bT_i^{l4} - aT_g - bT_w^4 \tag{12}$$

$$\underbrace{\begin{bmatrix} 1 + 2\lambda & -\lambda & \dots & 0 \\ -\lambda & 1 + 2\lambda & -\lambda & \vdots \\ \vdots & -\lambda & \ddots & -\lambda \\ 0 & \dots & -\lambda & 1 + 2\lambda \end{bmatrix}}_A \underbrace{\begin{bmatrix} T_1^1 \\ \vdots \\ \vdots \\ T_i^{l+1} \end{bmatrix}}_X = \underbrace{\begin{bmatrix} -aT_1^0 - bT_1^{04} - aT_g - bT_w^4 \\ \vdots \\ \vdots \\ -aT_i^l - bT_i^{l4} - aT_g - bT_w^4 \end{bmatrix}}_B \tag{13}$$

All terms on the right-hand side of equation 12 are known. Hence, the equation 12 forms a tridiagonal linear system. TC stem temperature (matrix X) can be calculated by multiply matrix B to inverse matrix of A .

The physical domain of thermocouple stem was discretised into 100 nodes and a code was written in Matlab to solve the above matrix. Shown in figure 2 is an example of the predicted temperature profile alongside the thermocouple stem generated by the model. The figure shows the difference between the indicated temperatures (thermocouple tip temperature) and the actual gas temperature (the red line in figure 2). In this example, a 0.5 mm diameter (K type) thermocouple with stainless steel 310 sheath (thermal conductivity 13 W/m.K) was placed at the centre of a 15 mm (internal diameter of 12 mm and 1.5 mm wall thickness) pipe. The TC was attached to the tube wall and had a perfect thermal contact with the wall. The TC length was 6 mm. The TC emissivity was set at 0.1 and the air velocity was 6 m/s. The air and wall temperature was 650 °C and 550 °C respectively. The graph shows that the TC tip temperature was at 634.6 °C but the actual air temperature was at 650 °C. In other word, the temperature measurement in this condition had 15.4 °C error. The modelling results were compared with the results reported by [1] (1) and there were good agreement between the reported results.

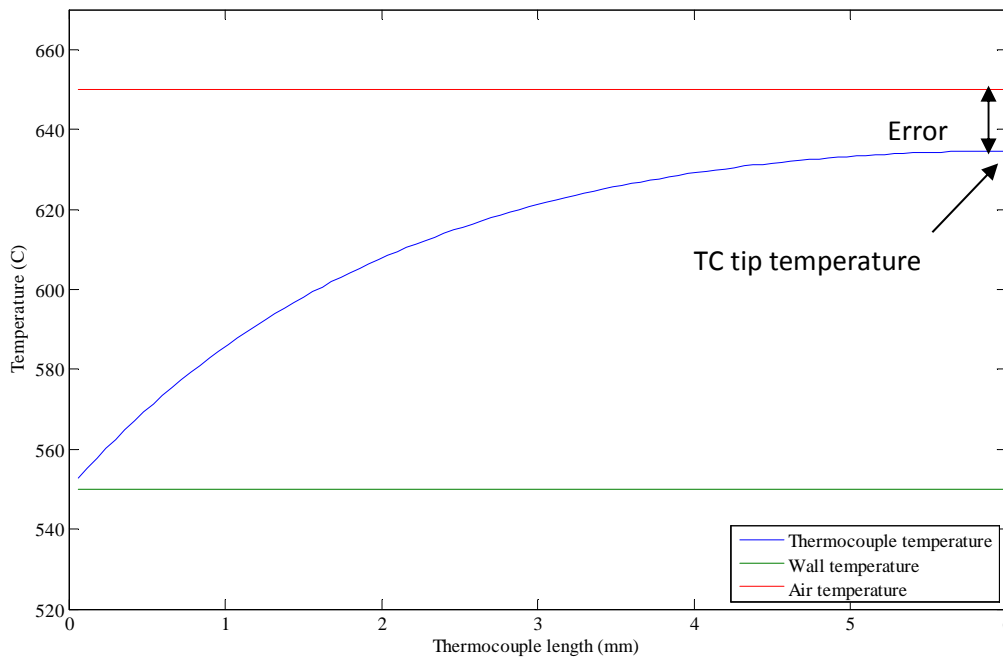


Figure 2 An example of temperature variation in a TC stem.

4. Design of Experiment

Design of Experiment (DOE) technique was performed to identify the key variables which affect the temperature measurement process and to determine at what levels these factors must be kept to reduce the measurement error. The results of the experiment were analysed and plotted using Minitab software.

In order to see the effect of different variables, four different scenarios and therefore four DOEs were considered. Figure 3 shows the first two scenarios. For the first scenario, a TC attached to a 15 mm (1.5 mm wall thickness) pipe with 6 mm exposed length inside the pipe. For the second scenario, a TC attached to a 25 mm (2 mm wall thickness) pipe with 10.5 mm exposed length. In figure 4, the TC

fitting moved 10 mm away from the pipe. Therefore, for the third and fourth scenarios, TC exposed length were 17 mm and 22 mm for 15 mm and 25 mm pipes respectively.

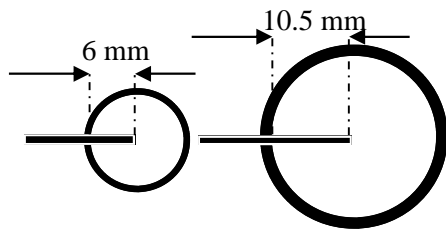


Figure 3. TCs attached to a 15 mm and 25mm pipe.

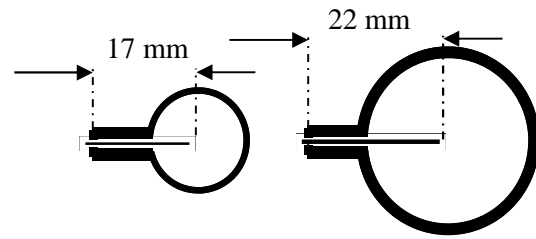


Figure 4. TCs attached to a 15 mm and 25mm pipe with 10mm extension.

The following tables (Table 1, 2) show the four scenarios and the factors/levels considered in this study. Two temperature levels, Low and high, were considered. The lower range, 550 °C – 650 °C, represents a nominal operating temperature range for metal-supported SOFC modules. Tabulated emissivity for stainless steel 316 is available in literature [11] but it varies depending on the condition of the surface, wave length, the exposed temperature and time. In general it could be 0.5 - 0.7 depends on finished surface and surface oxidation. One should bear in mind that TC emissivity increases by increasing temperature due to oxidation. It was reported that the polished stainless steel at room temperature has emissivity of 0.16 however by increasing the temperature to 1027 °C the emissivity could increase to 0.8 [8]. However, the emissivity could be kept at lower value by coating the TC surface. Therefore in this study a range of 0.1 to 0.7 was adapted to study the effect of emissivity in temperature measurement error. In addition to the above factors, two different TC diameters, 0.5 mm and 1.5 mm were studied. Thermocouple diameter could affect the heat transfers to thermocouples via conductivity (cross section area), radiation (effective surface area) and convection (exposed surface area).

Table 1. List of factors considered and their level for low thermocouple length

Factor	Labels	Scenario 1		Scenario 3	
		Low-level	High-level	Low-level	High-level
T_W (°C)	A	550	650	750	850
T_G (°C)	B	550	650	750	850
V_g (m/s)	C	6	40	6	40
ε	D	0.1	0.7	0.1	0.7
L_{TC}	E	6	10.5	6	10.5
D_{TC} (mm)	F	0.5	1.5	0.5	1.5

Table 2. List of factors considered and their level for high thermocouple length

Factor	Labels	Scenario 2		Scenario 4	
		Low-level	High-level	Low-level	High-level
T_W (°C)	A	550	650	750	850
T_G (°C)	B	550	650	750	850
V_g (m/s)	C	6	40	6	40
ε	D	0.1	0.7	0.1	0.7
L_{TC}	E	17	22	17	22
D_{TC} (mm)	F	0.5	1.5	0.5	1.5

Full factorial (two levels or one degree of freedom) design with six factors was considered for each scenario. The design matrix had 64 rows (2^6) and 6 columns. The design matrix then imported to the model and the estimated thermocouple errors (the temperature difference between the gas and the TC tip) were modelled for each 64 runs. The response matrix (estimated thermocouple errors) then exported to Minitab software to run the DOE analysis.

5. Results and discussion

Having obtained the results from the model, the first step was to compute the effect of factors and their interaction effects. The main effect is the difference in average response due to changes in the level factor. Shown in figure 5 is a graph of the main effects of the single variable affecting temperature measurement error in scenario 1. This plot demonstrates the factors influencing the temperature measurement error and it also shows the level of strength of each factor. In order to plot these graphs the mean response (measurement error) at each factor level was computed and then connected by a straight line. The reference line was drawn based on the overall mean of the response. The slope of the line indicates the effect of that factor on the results. If the slope is close to zero, then it means that there is no major effect presents. For instance in figure 5, the gas and the wall temperature had little effect on temperature measurement error. However, the graph shows that less error predicted for low wall temperature and high gas temperature. The reason for this behaviour was higher wall temperature causes a larger error due to conduction and radiation effect from the wall. The graph shows that TC diameter was the most important factor which affects the measurement error followed by TC length, Gas velocity and TC emissivity. The graph shows that increasing the TC diameter increases the measurement error due to having higher surface area for radiation and larger cross section area for higher thermal conductivity. It can be seen from the graph that increasing the TC length decreases the error due to lowering the TC stem effect (heat transfer through from the wall through the TC stem to the TC tip). The result also shows that increasing the gas velocity reduces the error. The actual gas temperature is measured by measuring the gas thermal energy transferred from/to the TC's tip by the convection and any other heat transfers from the adjacent components such as pipe wall would influence the measurement accuracy. Therefore, at high gas velocity the effect of convection is more dominant which reduces the effect of radiation and conduction effect on temperature measurement.

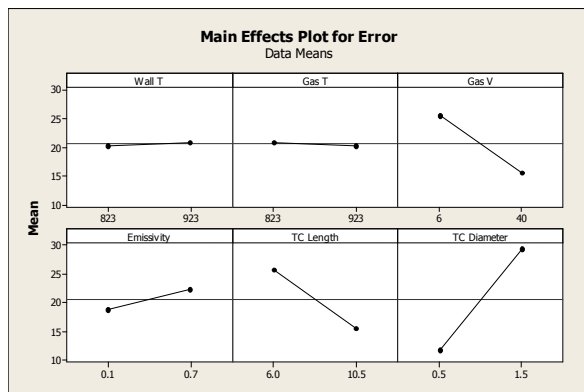


Figure 5. Main effects plot of the significant effects for scenario 1(temperature in K).

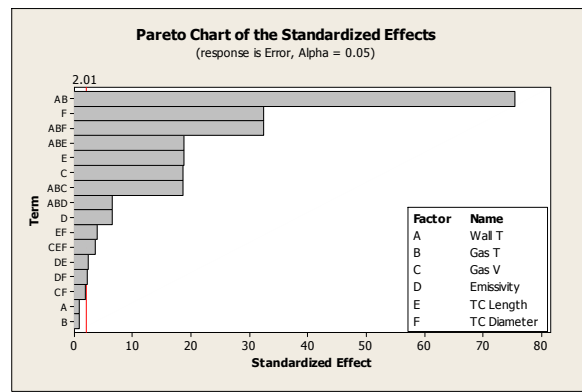


Figure 6. Pareto plot of factor effects for scenario 1.

Figure 6 shows the Pareto plot of the main effects and their combination. To generate this graph, the single and combined factors were analysed and the initial plot was produced. Then, the statistically insignificant factors and the combined factors, which were more than three single factors, were eliminated from analysis and process was iterated again. The final Pareto graph, which can be seen in Figure 6, was plotted to investigate significant of the factors and their interactions. The factors which

were lower than the red line (5% statistically significant level) were statistically insignificant. It can be seen for the graph that all the single factors excluding wall and gas temperature were significant. The graph also shows that the wall and gas temperature were insignificant factors; however, their combine factor (AB) was the highest. The next combined significant factor was ABF followed by ABE. This indicates the importance of factor F and E in this scenario. The single factor C was the next single important factor after E followed by the combined factor ABC and ABD. This shows that the emissivity factor, D, was the least significant single factor for this scenario.

Shown in figure 7 and 8 are the DOE analysis for scenario 2. In this scenario the length of the TC inside the pipe increased by 10 mm. Both graphs show that after increasing the TC length, the D factor was the most significant single factor followed by F, C and E. This shows that although the temperature range was similar to scenario 1, the emissivity factor became the most significant factor by increasing the TC length. In other words, by increasing the TC length, the error due to TC stem effect was reduced and the error due to radiative heat became a dominant factor in this scenario. Since the TC diameter also related to radiate heat transfer, it became the next significant factor. The graph shows that increasing the gas velocity reduces the error. By increasing the gas velocity, the Nusselt number also increases (equation 3) and consequently increases the heat transfer rate to the TC. This makes the convection more dominant than the other heat transfer mechanisms and reduces the temperature measurement error. The velocity effect can also be seen in figure 8 which shows that C, ABC, CF and CD were the significant factor next to D.

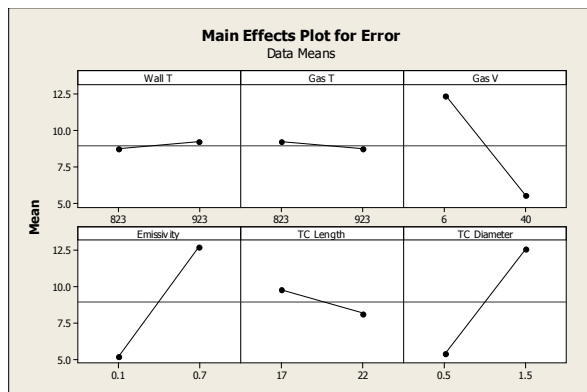


Figure 7. Main effects plot of the significant effects for scenario 2 (temperature is in K).

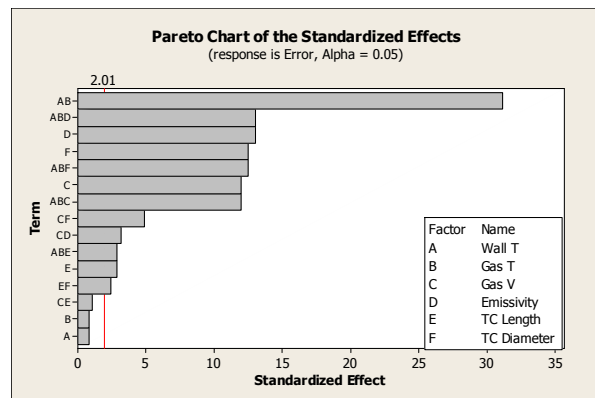


Figure 8. Pareto plot of factor effects for scenario 2.

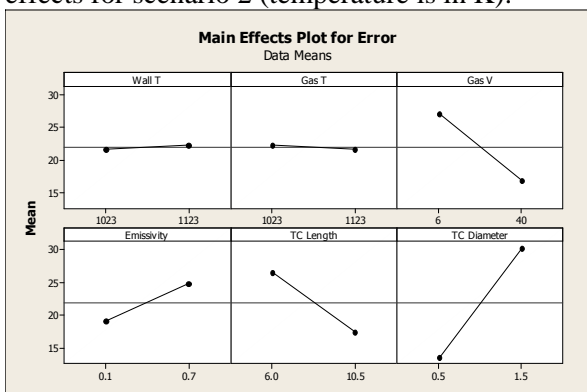


Figure 9. Main effects plot of the significant effects for scenario 3 (temperature is in K).

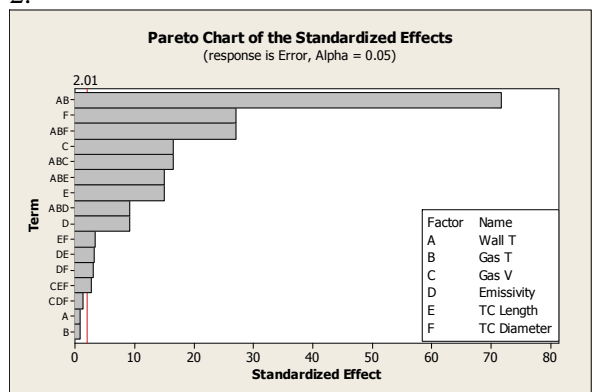


Figure 10. Pareto plot of factor effects for scenario 3.

Figure 9 and 10 show the DOE results for scenario 3. Although in scenario 3 the temperature range was 100 °C higher than scenario 1, D was the least single factor effect. This means that the TC stem

effect (combination of E and F) was dominant source of error in both scenarios (1 and 3). Despite the similarity between scenario 1 and 3, the errors (Standard Effect) for various factors were higher in scenario 3 than scenario 1.

The DOE results for scenario 4 were depicted in figure 11 and 12. The results show that D was the most significant single factor and E was the least significant single factor affecting the temperature measurement error. This was similar to the results were obtained from scenario 2. The gas velocity, C, was the second highest significant single factor in scenario 4 but in scenario 2 F was the second highest significant factor. Despite this difference in scenario 1 and 4, the difference between C and F were not significant for both scenarios. This means that D, C and F were significant factors affecting the temperature measurement regardless of the operating temperature when the TC length was longer than scenario 1 and 3.

As discussed earlier, some of the assumptions such as thermal conductivity (between and the TC and fitting), TC emissivity and flow profile are not fully representative of the real world. Therefore, the DOE and modelling results require experimental validation. A test rig has been manufactured and the results and comparison with the DOE model will be reported in a future paper.

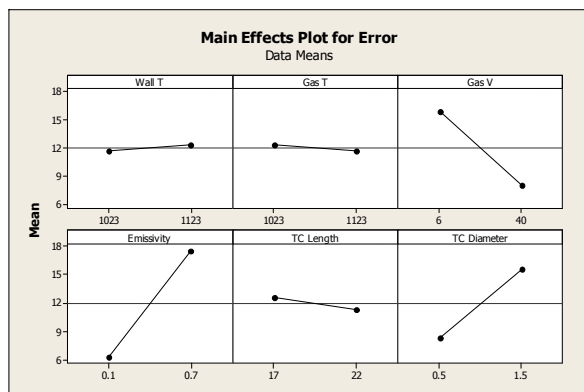


Figure 11. Main effects plot of the significant effects for scenario 4 (temperature is in K).

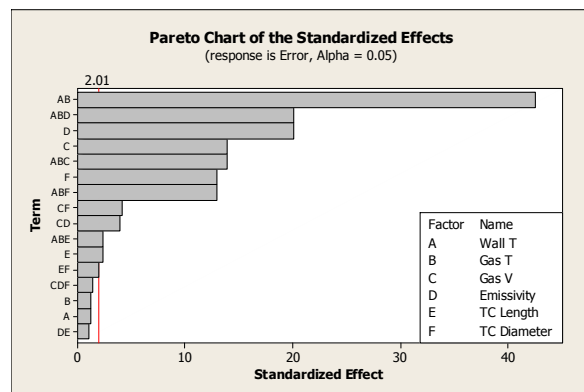


Figure 12. Pareto plot of factor effects for scenario 4.

6. Concluding remarks

A one-dimensional mathematical model was developed and numerically solved to investigate the temperature measurement error for a thermocouple placed at a centre of a pipe to measure the flow temperature. DOE method was applied to the modelling results to investigate the key variables affecting the temperature measurement. Four temperature measurement scenarios were proposed based on conditions similar to those found in metal-supported SOFC. One scenario was the TC length was equal to the half of the pipe internal diameter and the second scenario was extending the TC length for 10mm. Both scenarios were analysed at two different temperature ranges. One for SOFC stack temperature (550 °C – 650 °C) and the other was for the gas temperature after the burner (750 °C – 850°C). In this study a full factorial design at two levels for six variables was considered for each scenario. The DOE results for each scenario were reported and analysed. The results showed that for short TC length, TC diameter and TC length were the most significant factors even at higher temperature range. By extending the TC length, TC emissivity and gas velocity became significant factors even at lower temperature range.

Acknowledgements

The authors wish to thank Knowledge Transfer Partnership (KTP), Technology Strategy Board (TSB), University of Brighton and Ceres Power Ltd for their funding of this project.

References

- [1] Tsikonis L, Van herle J and Favrat D 2012 The Error in Gas Temperature Measurements with Thermocouples: Application on an SOFC System Heat Exchanger *Fuel Cells* **12** 32-40
- [2] Villafañe L and Paniagua G 2013 Aero-thermal analysis of shielded fine wire thermocouple probes *Int.l J. of Thermal Sci* **65** 214-223
- [3] Yilmaz N 2011 Detailed multiphysics modeling and validation of thermocouple readings in fires *J. of Fire Sci* **29**(5) 443-464
- [4] Roberts I L and Coney J 2011 Estimation of radiation losses from sheathed thermocouples *Appl Thermal Eng.* **31** 2262-2270
- [5] Blevins L G and Pitts W M 1999 Modeling of bare and aspirated thermocouples in compartment fires *Fire Safety J.* **33** 239-259
- [6] Rizika J W and Rohsenow W M 1952 Thermocouple Thermal Error *Eng. and Pro. Development* **44**(5) 1168-1171
- [7] Yilmaz N 2012 Effect of thermocouple insertion depth in multiple directions on temperature measurements *J. of Fire Sci* **30**(3) 201-210.
- [8] Incropera F P, Dewitt D P, Bergman T L and Lavine A S 2013 *Principles of Heat and Mass Transfer* 7th ed. (Singapore: John Wiley & Sons) p796
- [9] Kadoya K, Matsunaga N and Nagashima A 1985 Viscosity and thermal conductivity of dry air in the gaseous phase *J. Phys. Chem. Ref. Data* **14** 947-9770
- [10] Asadi M and Haghghi Khoshkho R 2013 Temperature Distribution along a Constant Cross Sectional Area Fin *International Journal of Mechanics and Applications* **3** 131-137
- [11] Cao G, Weber S J, Martin S O, Sridharan K, Anderson M H and Allen T R 2013 Spectral emissivity of candidate alloys for very high temperature reactors in high temperature air environment *J. of Nuclear Materials* **441**(1-3) 667-673